

12-2017

Graphene field effect transistors for highly sensitive and selective detection of K⁺ ions

Hongmei Li

Clemson University, hongmel@clemson.edu

Yihao Zhu

Clemson University

Md. Sayful Islam

Clemson University

Md. Anisur Rahman

University of South Carolina

Kenneth B. Walsh

University of South Carolina

See next page for additional authors

Follow this and additional works at: https://tigerprints.clemson.edu/elec_comp_pubs



Part of the [Electrical and Computer Engineering Commons](#)

Recommended Citation

Please use the publisher's recommended citation. <http://www.sciencedirect.com/science/article/pii/S0925400517311486>

This Article is brought to you for free and open access by the Holcombe Department of Electrical & Computer Engineering at TigerPrints. It has been accepted for inclusion in Publications by an authorized administrator of TigerPrints. For more information, please contact kokeefe@clemson.edu.

Authors

Hongmei Li, Yihao Zhu, Md. Sayful Islam, Md. Anisur Rahman, Kenneth B. Walsh, and Goutam Koley

Graphene field effect transistors for highly sensitive and selective detection of K^+ ions

Hongmei Li¹, Yihao Zhu², Md Sayful Islam¹, Md Anisur Rahman³, Kenneth B. Walsh⁴ and Goutam Koley¹

¹Department of Electrical and Computer Engineering, Clemson University, SC 29634, U.S.

²Department of Electrical and Computer Engineering, University of South Carolina, Columbia, SC 29208, U.S.

³Department of Chemistry and Biochemistry, University of South Carolina, Columbia, SC 29208, U.S.

⁴Department of Pharmacology and Neuroscience, University of South Carolina, Columbia, SC 29209, U.S.

Corresponding author: Hongmei Li

E-mail: hongmel@clemson.edu, Address: 91 Technology Dr. Lab 59A, Anderson, SC 29625, U.S

Abstract. Graphene-based ion sensitive field effect transistors (GISFETs) with high sensitivity and selectivity for K^+ ion detection have been demonstrated utilizing valinomycin based ion selective membrane. The performance of the GISFET for K^+ ion detection was studied in various media over a concentration range of 1 μ M – 2 mM. The sensitivity of the sensor was found to be > 60 mV/decade, which is comparable to the best Si-based commercial ISFETs, with negligible interference found from Na^+ and Ca^{2+} ions in high concentration. The sensor performance did not change significantly in Tris-HCl solution or with repeated testing over a period of two months highlighting its reliability and effectiveness for physiological monitoring. The performance of the sensor also remained unchanged when fabricated on biocompatible polyethylene terephthalate (PET) substrate, showing significant potential for developing flexible bio-implantable graphene-based ISFETs.

Keywords: Graphene; Ion sensitive field effect transistor; K^+ ion detection; ion selective membrane

1. Introduction

Sensors based on Graphene, exploiting its outstanding material properties, including remarkably high charge carrier mobility [1], very high surface to volume ratio, and very low Johnson noise [2], are currently of strong technological interest in chemical, electrical and even in bio sensing application [3] since the adsorbed molecules can readily affect its conductivity through charge transfer [2, 4]. Graphene, being essentially a surface, is extremely sensitive to changes in surface charge, or interaction with ionic adsorbates, presenting itself as an excellent material to develop ion sensitive field effect transistors (ISFETs). The vast majority of the ISFETs demonstrated so far focus on the detection of H^+ ions utilizing various surface functionalization layers [5, 6]. Although somewhat more challenging, due to the requirement of selective functionalization layers, detection of metal ions (especially those of alkali metals) are of high significance due to their important role in cell physiological processes.

Elevations in biological levels of K^+ ions precede the onset of sudden cardiac death, epileptic seizures and other clinical problems [7, 8]. However, the time course and magnitude of these changes in extracellular K^+ ions is yet unknown. Therefore, the development of implantable K^+ -sensitive sensor devices could be of great use in predicting the onset of myocardial infarctions and seizures. In addition, ISFETs present a noninvasive and bio-compatible technology for measuring

K^+ efflux from primary and stem-cell derived cells that are used for toxicological and drug discovery testing.

Si-based ISFETs are already commercially available, although they suffer from several drawbacks. One of the major challenges with the Si-based ISFETs is that ions (i.e. H^+ , OH^-) typically migrate into the oxide (accumulating at the SiO_2/Si interface) and change the threshold voltage of the FET [9, 10], leading to their degradation over time with repeated usage. Graphene offers an excellent opportunity to address this limitation of Si-based sensors offering a surface that is impervious to ions. Even more significantly, graphene synthesized by chemical vapor deposition (CVD) on Cu foil can be transferred to various substrates of choice (other than SiO_2/Si), which helps to avoid this issue of ion accumulation and associated device degradation completely (demonstrated in this work by realizing graphene ISFET on PET substrate).

In this article, we present a highly sensitive and selective graphene-based ISFET (GISFET) capable of detecting K^+ ions down to $1 \mu M$ (utilizing valinomycin based membrane coating), showing excellent selectivity with respect to common interfering Na^+ and Ca^{2+} ions at several orders of magnitude higher concentration. The feasibility of using graphene-based ISFETs for bio-implantable applications was also studied by testing them in Tris-HCl solution and fabricating them using PET substrate, which is inert and highly bio-compatible. The devices showed high repeatability and reliability in sensing experiments conducted over a period of two months.

2. Experimental

2.1. Graphene growth

Graphene samples used to fabricate the ISFETs were synthesized using chemical vapor deposition (CVD) in a semi-automated quartz tube furnace system as discussed in detail elsewhere [4, 11]. Briefly, monolayer, uniform graphene over a large area was grown on a copper foil (Alfa Aesar, 99.999% purity), which acted both as the substrate and catalyst. Methane was used as the growth precursor, along with H_2 and Ar as the carrier gases, which were flown into the furnace using mass flow controllers (MFCs, MKS Instruments) at nominal flow rates of 100, 100 and 900 sccm, respectively. The copper substrate was annealed at $1000^\circ C$ for 2 hours under a continuous flow of H_2 and Ar gases prior to growth, which was followed by the graphene growth at $1035^\circ C$ over a duration of 20 mins under a continuous flow of methane.

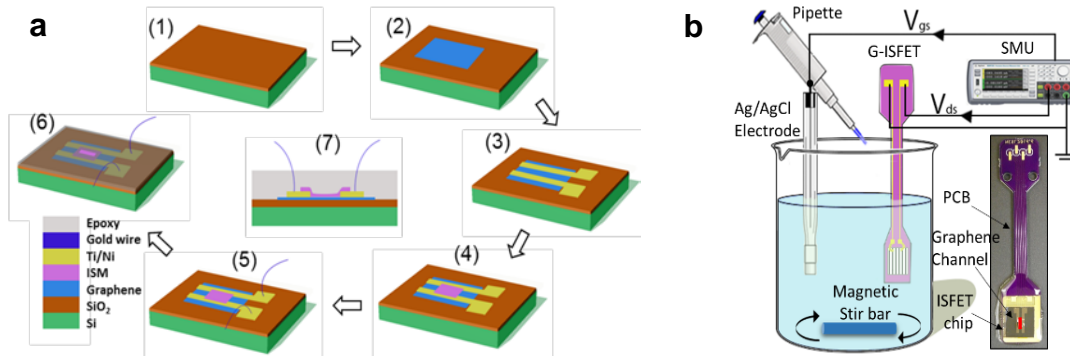


Fig. 1 ISFET fabrication process flow and measurement set up. **a)** ISFET chip fabrication steps. 1. Substrate preparation. 2. Graphene transfer. 3. Source and drain formation. 4. ISM coating. 5. Mounting chip to PCB. 6. Epoxy encapsulation. 7. Schematic diagram of G-ISFET chip cross-section. **b)** Ion concentration sensing set up. Picture of real ISFET device (right bottom), with the sensor chip mounted on PCB head.

2.2. GISFET chip fabrication

Graphene films synthesized on Cu foils were used to fabricate GISFET devices following a sequence of processing steps as discussed below (Fig.1 (a)). To begin with, the Cu foil with graphene film was coated with polymethyl methacrylate (PMMA) using a spin coater, and baked for 1 minute at 150 °C. Next, the graphene layer on the back side of the sample was removed by oxygen plasma etching (Plasma Etch, PE25-JW-HF), which was followed by Cu etching in ammonium persulfate solution for over 3 hours, releasing the graphene/PMMA top layer. After rinsing in deionized water, the graphene/PMMA layer was transferred and placed on SiO₂ (300 nm)/Si (n⁺ doped) substrate in isopropyl alcohol and allowed to dry for 15 minutes. Finally, the sample was dipped in acetone for 4 hours to remove PMMA. To fabricate GISFETs, Ti (30 nm)/Ni (150 nm) source/drain contacts were deposited on the transferred graphene using an electron beam evaporator, with the contact areas defined by a metal mask. The graphene channel formed had dimensions of 2 x 1 mm. We used high-quality SiO₂ grown through a dry thermal oxidation process to minimize any leakage current between the metal contacts and the silicon substrate. To determine their material quality, the graphene films were characterized using Raman spectroscopy (Renishaw Raman system, InVia) and atomic force microscopy (D3100 from Veeco).

2.2.1. Valinomycin based ion selective membrane preparation

To perform selective detection of K⁺ ions, valinomycin (C₅₄H₉₀N₆O₁₈) based ion selective membrane (ISM) with 5 μm nominal thickness was spin-coated on the entire transferred graphene area and kept at room temperature for 20 minutes for complete solvent volatilization and stable film formation. The K⁺ ISM was prepared [12] by dissolving 8 mg valinomycin (VAL), 1.10 mg potassium tetrakis (4-chlorophenyl) borate (K-TCPB), 390 mg acrylic matrix copolymer (made of methyl methacrylate (MMA) and n-butyl acrylate (nBA) monomers in the proportion of 1:10) [13] in 2.0 ml of tetrahydrofuran [14].

To ensure optimum device performance and reliability, we have developed a self-plasticized methacrylate and nBA based copolymer. This block copolymer is a two-phase system (please refer to Fig. S1); mostly containing nBA, which consists of continuous amorphous phase through which molecular transportation occur rapidly, while the methacrylate block forms a discontinuous, crystalline phase that cross-links the structure. In addition, the higher molecular weight of 151,000 Da (Fig. S2) of methacrylate and nBA copolymer provide sufficient polymer chain entanglement to make the membrane more mechanically robust in harsh operating conditions, while maintaining very low predominant glass transition temperature (-43.05 °C) (Fig. S3) that enables easy ion transportation across the membrane towards the graphene surface [15].

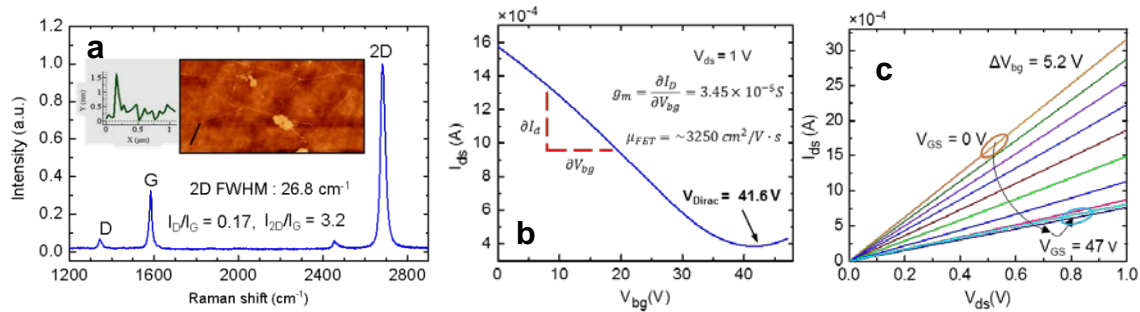


Fig. 2 Graphene characteristics. **a**) Raman spectroscopy of graphene transferred on SiO₂ showing good quality. The right inset figure is the AFM image, exhibiting smooth graphene layer surface and folds. The left inset figure is shown a line profile of graphene AFM image. **b**) Graphene FET mobility extraction. Graphene's $I_d - V_{bg}$ characteristic is measured from graphene FET device; the plot showing graphene's typical V-shaped characteristics. **c**) A family of $I_{ds} - V_{ds}$ plots is shown with varying back gate voltage (V_{bg}).

Furthermore, mobile cation-exchange sites such as potassium tetrakis (4-chlorophenyl) borate [K-TCPB] has been dispersed in the polymer membrane, which reduces the membrane resistance and activation barrier for the cation-exchange reaction at the membrane/solution interface resulting in a significant reduction in ionic interfaces, thereby increasing the ion-detection sensitivity [16 – 18]. Taken together, the polymer membrane formulation uniquely offers all the necessary attributes for a highly sensitive, selective, reliable non-plasticized polymer membrane for biomedical and solid-state microfabrication ion sensors.

The valinomycin structure consists of alternately bound amide and ester bridges (shown as inset of Fig. S4 of supplementary data). The presence of the carbonyl group, coupled with its unique doughnut-shaped structure enables valinomycin to easily bind metal ions. Due to the size of the potassium ion (1.33 Å radius), valinomycin exhibits a very high stability constant ($K = 10^6$) toward it compared to other metal ions. This results in a high degree of selectivity compare to other complexes; i.e. Na^+ with 0.95-angstrom radius forms 10,000 fold weaker valinomycin- Na^+ complexes, and thus valinomycin is 10,000 more times selective to K^+ [19]. While the K^+ by itself is able to cross single lipid bilayer, it has been shown that the presence of valinomycin in the lipid layers makes it freely permeable through multiple lipid bilayers [20]. This property was utilized in our design of the ion selective layer to make it specifically permeable to K^+ ions. Another important advantage of using valinomycin is that it can act as a functionalization layer on the graphene surface of the ISFET enhancing its sensitivity. Since pristine graphene is chemically inert [21], many research groups have adopted different kinds of oxide layers (SiO_2 , HfO_2 [22], Ta_2O_5 [23]) as well as aromatic molecules as a functionalization layer on top of the graphene surface to enhance its ion sensing capabilities. The valinomycin layer coated on the graphene surface can enhance the ISFET sensitivity, similar to other aromatic molecule functionalizations [24, 25].

2.2.2. Encapsulation.

For stable operation in an electrolytic environment, the GISFET chip was mounted on a printed circuit board (PCB) and the source/drain ohmic contacts were wire bonded to the contact pads on the PCB. To isolate and protect the metal contacts and the bonding wires from the conducting aqueous environment, epoxy glue (Epo-tech 301) was used to encapsulate them. The selected epoxy is biocompatible and specially designed for medical electronics with USP Class VI and/or ISO-10993 compliance. After careful mixing of epoxy resin and curing agent (4:1), the mixture was applied to the metal contact, SiO_2/Si chip and bonding wires, leaving a small window (2×1 mm in dimension) on the ISM coated graphene (see above discussion) as the active sensing area (to be in contact with the test solution), and cured for 2 hours at 60 °C on a hot plate. Inset of Fig. 1 (b) shows the optical image of a GISFET after encapsulated by epoxy.

Figure 1(a) shows a summary of the processing steps involved in the fabrication of the GISFET device, while Fig. S4 shows a schematic summarizing the operation of the ion-selective membrane.

2.3. GISFET electrical properties and performance recording methods

The electrical characteristics of the fabricated graphene FET and GISFET were studied thoroughly and systematically in the air and in an electrolytic solution, respectively. Carrier mobility was measured using a back-gated FET configuration, while Hall mobility measurements were carried out using an HMS 3000 (Ecopia) system. The experimental setup for measurements in the electrolytic solution is schematically illustrated in Fig. 1(b). The Ag/AgCl reference electrode was used to apply a top-gate bias for obtaining the $I_{\text{ds}}-V_{\text{tg}}$ characteristics of the GISFET in solution. For the I-V measurement, dc bias for V_{ds} and V_{gs} were supplied by a precision source measure unit (SMU, Keysight B2902A), while simultaneously measuring I_{ds} . The device response was studied by varying the K^+ ion concentration from 1 μM to 20 mM in distilled water, in Tris-HCl solution, as well as in 140 mM NaCl solution (imitating the Na^+ ion concentration in a typical physiological solution). Test electrolytes with desired ionic concentrations were realized using carefully prepared stock solutions transferred using micropipettes. The measured $I_{\text{ds}} - V_{\text{tg}}$ curves show typical V-

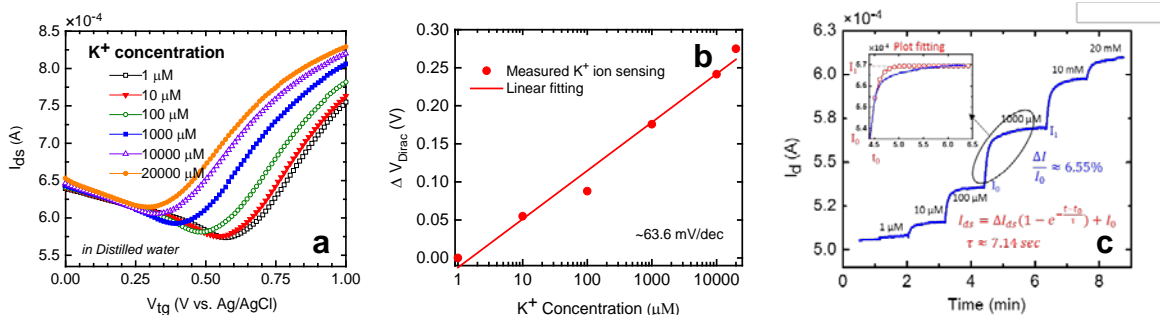


Fig. 3 K^+ sensing characteristics of GISFET. **a)** K^+ sensing in distilled water based electrolyte solution. Dirac points can be seen to shift very significantly as the K^+ concentration increases from 1 μM to 20 mM. **b)** Dirac point shift varies with K^+ concentration change fairly linearly, showing an average sensitivity of ~ 64 mV/dec for the least square fit. **c)** Current change response as the by K^+ concentration was changed in steps from distilled water to 20 mM. Fractional change in current used to calculate sensitivity and time constant for sensing response are calculated from exponential fits to the response transients corresponding to each concentration change.

shaped I-V characteristic underlining sharp transition from p- to n-type graphene upon application of top-gate bias.

3. Results and discussion

3.1. Structural characterization

Figure 2(a) shows a typical Raman spectrum for our samples with signature D, G and 2D peaks. The I_D/I_G ratio of ~ 0.17 indicates good quality of the graphene layers [26]. The 2D peak full width at half maximum (FWHM) value of ~ 26.8 cm^{-1} , and the intensity ratio of the 2D band (at 2682 cm^{-1}) and G band (at 1585 cm^{-1}) was 3.2, indicating the presence of a single layer of monolayer graphene [27]. The inset of Fig. 2(a) shows an atomic force microscopy (AFM) morphology image ($2.5 \mu\text{m} \times 5 \mu\text{m}$) taken from a transferred graphene film after undergoing an annealing process, which was carried out in a quartz tube at 400°C for 2 hours in the forming gas environment to remove any residue of PMMA. The AFM image showed smooth and continuous graphene layer, exhibiting folds that are commonly observed after transfer [11].

3.2. Electrical characterization GISFETs

Charge carrier mobility is an important parameter directly affecting the sensitivity of the graphene ISFET device. Therefore, we measured back-gated FET mobility, and hall mobility before moving on to GISFET device fabrication. For measuring FET mobility, Ti/Ni metal stacks were deposited on the transferred graphene to form source and drain contacts, with a graphene channel of dimensions of 2.8×1.5 mm between them. The highly doped silicon substrate was used as the back gate with 300 nm SiO_2 as the insulator layer. The $I_{ds} - V_{bg}$ plot (see Fig. 2 (b)) is ambipolar in nature which is a direct consequence of linear dispersion relation in graphene with zero band gap. The Dirac point was observed at $V_{bg} = 41.6$ V. A positive Dirac point indicates that CVD grown graphene transferred on SiO_2 is p-type in nature, which is expected and commonly observed [28, 29]. The Fig. 2(c) plot shows a linear $I_{ds} - V_{ds}$ family of curves where the back-gate bias varies from 0 to 47 V at a V_{bg} increment of 5.22 V. A good back gate modulation was observed (supporting expected p-type graphene behavior), and the FET hole mobility was calculated using the formula $\mu_{FET} = (g_m L)/(WC_{ox}V_{DS})$ [30]. Here g_m is the transconductance ($\partial I_{DS}/\partial V_{GS}$) at the p-type graphene side, L and W are the length and width of the graphene channel, respectively, and C_{ox} is the oxide capacitance per unit area. Using an extracted g_m value of 3.45×10^{-5} S from the $I_{ds} - V_{ds}$ characteristic, the mobility was found to be 3,250 cm^2/Vs , which is comparable to the mobility of typical high quality graphene transferred on SiO_2 [31, 32].

Hall mobility measurement was also carried out on the same graphene sample and compared to the FET mobility. To measure Hall mobility, 6×6 mm square shape graphene film was transferred on the SiO_2 substrate, and simple indium press contacts were established on each of the four corners of the sample. The Hall mobility of the graphene sample was measured to be $2660 \text{ cm}^2/\text{Vs}$ which is comparable to the FET mobility extracted above, with the reduction attributable to the bigger size of the graphene layer used for Hall measurements (6×6 mm) compared to FET (1.5×2.8 mm), which exhibits an average mobility over a larger area that is typically smaller.

3.3. GISFETs measurements of K^+ ionic concentration in distilled water

After fabrication of the GISFET, we performed detailed electrical characterization and investigated the K^+ sensitivity of the GISFET in a distilled water based K^+ ion solution. The variation in drain current with top gate voltage ($I_{\text{ds}} - V_{\text{tg}}$ characteristics) was measured using a standard Ag/AgCl reference electrode (where the gate voltage was applied), in a test electrolyte solution of variable KCl concentration, and the results are plotted in Fig. 3(a). The Dirac point in the $I_{\text{ds}} - V_{\text{tg}}$ plots can be seen to vary from $0.2 - 0.7$ V, which is a dramatic reduction compared to the Dirac point of ~ 40.6 V measured for the same FET in air prior to valinomycin coating [please refer to Fig. 2(b)]. This large change in Dirac point can be attributed primarily to the strong electron donating nature of the valinomycin molecule which possesses 6 amides ($\text{RnE(O)xNR}'_2$) functional groups. Indeed, separate experiments conducted on back gated FETs in ambient conditions indicate that a large Dirac point shift, by $20 - 30$ V, can be caused by valinomycin coating, which donates electrons to p-type graphene to shift the Dirac point closer to 0 V. Another important point to note here is that the high capacitance of the electrical double layer (EDL), formed at the interface of graphene and the electrolytic solution [33], enables the ISFET device to operate at a much narrower voltage range (i.e. charge density and Fermi level changes much more rapidly with applied top gate voltage; g_m change from $\sim 10^{-5}$ S for back-gate FET to $\sim 10^{-4}$ S for top-gate FET), which offers a significant advantage for practical sensor design. Indeed, the capacitance for a back-gated FET can change by orders of magnitude from nF/cm^2 range in the air [closely matching our extracted capacitance of $11.5 \text{ nF}/\text{cm}^2$] to $\mu\text{F}/\text{cm}^2$ range in the electrolytic environment as shown by Ye et al [33]. From Fig. 3(a) we also observe that the Dirac points shifts very significantly, from 0.57 V to 0.29 V, as the K^+ concentration increases from $1 \mu\text{M}$ to 20 mM . Such a movement of the Dirac point to lower values is expected since the K^+ ions near or at the graphene surface induces higher electron concentration (i.e. reduces hole concentration in p-type graphene), thereby moving the Fermi level closer to the charge neutrality point, and consequently lowering the Dirac point. Such a lowering of Dirac point due to adsorption of positively charged ions is also observed commonly for H^+ ions in a pH ISFET [24, 34].

3.4. Sensitivity and response time

Since sensitivity and response time are two critical parameters for any sensor, we carefully examined these parameters for our graphene ISFETs. A commonly used method to determine the sensitivity of ISFETs (i.e. commercial Si ISFETs) is to look at the shift in threshold voltage (equivalent to the shift in Dirac point of the ISFET) as a function of the change in K^+ ion concentration [35]. The change in Dirac point as the K^+ ion concentration was varied from $1 \mu\text{M}$ to 20 mM (this includes the range of interest for cellular efflux of $10 \mu\text{M} - 1 \text{ mM}$ [36]) can be determined from Fig. 3(b) to be ~ 280 mV, and hence the sensitivity can be calculated as $64 \text{ mV}/\text{decade}$ ($= 280 \text{ mV}/4.3 \text{ decade}$), which is very comparable to that obtained from the Si-based ISFET devices [37].

Another method (commonly used for chemical sensors) to determine the sensitivity and the response time is to determine the magnitude and temporal variation of the ISFET drain current as the K^+ ion concentration is changed in steps. To this end, we recorded the I_{ds} as a function of time for various K^+ concentrations (for a fixed value of V_{tg}) using a data acquisition unit (DAQ, Keysight

34972A); and the results are shown in Fig. 3(c). A plot of the concentration change from 100 μM to 1 mM (corresponding to typical cellular efflux) is shown in the inset of Fig. 3(c) to calculate the response time and current change based sensitivity ($\Delta I/I$, similar to the sensitivity calculated for chemical sensors). As can be seen, the current changes from 528 to 563 μA , corresponding to a fractional change in current of $\sim 6.6\%$ per decade change in K^+ ion concentration. Fitting the time-dependent response plot with an exponential function, a time constant of $\tau \approx 7.1$ second can be extracted, which is very close to the best values of ~ 5 seconds observed for commercial pH sensors (Topac, S1600 Advanced pH meter).

3.5. Measurements of K^+ ionic concentration in Tris-HCl solution and high background Na^+ concentration

To determine the applicability of the GISFETs for K^+ ion measurements in physiological solution, its performance was investigated in a 0.1 M tris-HCl solution with pH 7.4 (from VWR), which is commonly used in buffer solutions for biochemistry and molecular biology experiments (i.e. Protein Electrophoresis, Western Blotting and Nucleic Acid Agarose Electrophoresis [38]). The results for K^+ ion sensing are illustrated in Fig. 4(a) where the Dirac point is found to shift by 0.275 V for a 4.3-decade change in K^+ concentration, exhibiting a sensitivity of 64 mV/decade, which is exactly same as that obtained for K^+ concentration variation in distilled water discussed above.

To further test the suitability of our sensor for usage in physiological solution, where typically very high (~ 150 mM) background concentration of Na^+ is present, we tested the performance of the device in concentrated NaCl solution (140 mM), and the results are shown in Fig. S6. The sensitivity is found to be 65 mV/decade in the sensing range of 10 μM - 20 mM, showing very similar sensitivity to the distilled water based solution. Below 10 μM , reliable sensing of the K^+ ion variation was found to be difficult as the high Na^+ concentration increased the K^+ ion sensing baseline (this is actually expected based on the expected selectivity of 10,000 for K^+ ions relative to Na^+ ions as discussed above). Nonetheless, the operational range of the sensor completely covers the concentration range of interest for cellular efflux measurements of 100 μM to 1 mM (see discussion above).

3.6. Ion selectivity of the GISFETs

Although graphene-based ISFETs have been extensively studied for pH sensing or Na^+ sensing [22, 39] by many research groups, the ion-selectivity aspect is generally not investigated in detail, although it is one of the most important characteristics of any sensor. In this research, we have

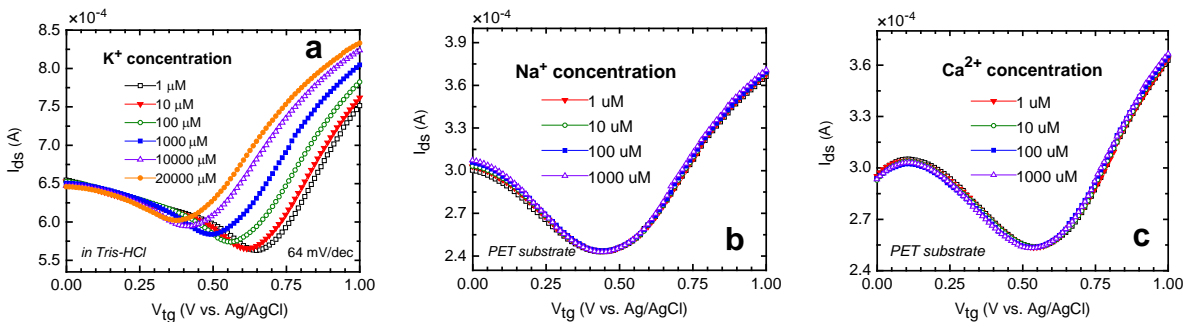


Fig. 4 GISFET's stable sensitivity in buffer solution, and its good selectivity. **a)** K^+ sensing in 0.1 M Tris-HCl solution (pH 7.4). The result shows good sensitivity exhibiting similar value as obtained from distilled water based solution. **b), c)** The GISFET with Valinomycin polymer matrix coating is effectively insensitive to Na^+ ions or Ca^{2+} ions over the concentration range of 1 ~ 1000 μM NaCl or CaCl_2 (measurement performed in distilled water-based solution), as can be inferred from the overlapping I-V plots.

made the ISFETs selective to K^+ ions by coating them with valinomycin based ISM. Details of the mechanism and preparation for the ISM coating have been discussed in experimental section as well as in the supplemental information section. In a device structure, when the device is interfacing with an electrolyte solution, valinomycin in ISM selectively traps only K^+ ion from the solution, forming a valinomycin- K^+ complex, which can further transit to the vicinity of graphene surface (as illustrated in Fig S1). The electrical field exerted from the captured K^+ ions affects the conductivity of graphene channel and thus induces an electrical sensing signal. The ion selectivity of the sensor was studied by comparing the responses of the ISFET to common background ions Ca^{2+} and Na^+ vis-a-vis the K^+ ions. Figure 4(b, c) presents the responses to Na^+ and Ca^{2+} ions over the range of $1 \mu\text{M} - 1 \text{mM}$. We found that even though the concentration of these ions changed by 3 orders of magnitude the Dirac point did not shift, clearly highlighting the high selectivity of our ISFET with respect to these interfering ions. In contrast, a large response was observed for K^+ ions in distilled water based solution and also in presence of high interfering ionic concentration (i.e. $140 \text{mM } Na^+$) as already discussed in detail above. This clearly underlines the high selectivity of the proposed ISFET sensor.

3.7. Repeatability and reliability of the GISFET device

For robust ion sensing applications, the ionic concentration measurements by the ISFET need be reliable and repeatable. To study this, the performance of a GISFET was recorded over a period of two months by periodically measuring its sensitivity to K^+ ion concentration. The results are shown in Fig. 5(a), which shows an average sensitivity of 61mV/dec over a course of two months with a standard deviation of 4.6mV/dec . It should be noted that the sensitivity of the device exhibits a range bound fluctuation over the course of the month instead of exhibiting any monotonically varying trend, which rules out steady degradation of the ISFET device over time, unlike widely observed for its Si counterparts⁸. The cause for such small fluctuations are still under investigation but likely contributed by randomly varying experimental and environmental factors. For a given measurement the ionic concentration was measured at least 3 times by the ISFET sensor, which was found to be highly repeatable, with only 1% deviation from the mean sensitivity value.

3.8. GISFET device on polymer substrate

Fabrication of ISFETs on flexible substrates is highly attractive for implantable biosensing applications. Unlike Si-based ISFETs, graphene is inherently compatible with flexible substrates due to its own flexible nature and easy transfer process of CVD graphene to various substrates without undergoing any cumbersome fabrication process. Polyethylene terephthalate (PET) is a material widely used for numerous applications involving our daily life [40] (i.e. in bottles,

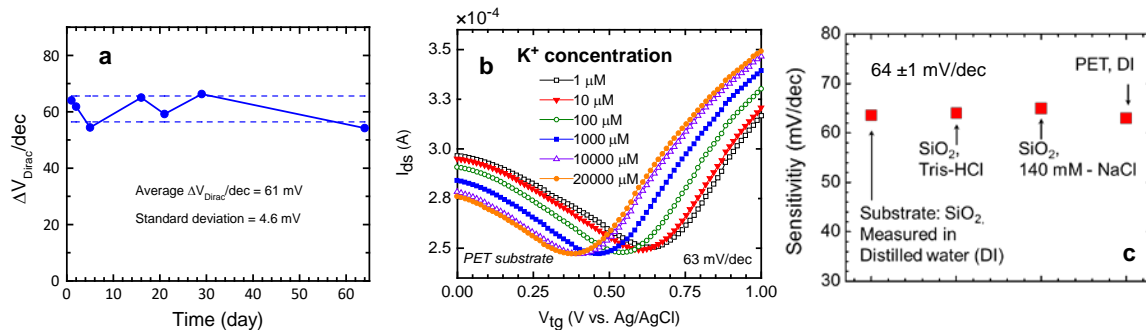


Fig. 5 GISFET's performance at different solution bases or fabricated on different substrates. **a)** Sensitivity of the GISFET sensor measured over a duration of two months shows a stable response with an average sensitivity of 61mV/dec and a standard deviation of 4.6mV/dec . **b)** GISFET fabricated on flexible substrate PET shows an average K^+ ion sensitivity of $\sim 63 \text{mV/dec}$ over the concentration range of $1 \mu\text{M}$ to 20mM . **c)** GISFET's stable sensitivity in different solution bases or fabricated on different substrates.

packaging materials etc.) due to its extremely low toxicity and low cost. It is also a material of choice for technical applications (i.e. automotive and electronics) owing to its excellent dielectric strength and chemical inertness [41]. In this work, we therefore investigated the feasibility of fabricating high-performance graphene-based ISFETs on PET substrate. The fabrication steps and materials used are very similar to the GISFET on SiO₂/Si substrate, except the substrate itself is replaced with PET. The performance of GISFET on PET was determined in the same way as discussed above, and the result is shown in Fig. 5(b). We find the K⁺ ion sensitivity to be ~63 mV/dec (= 272 mV/4.3 decade), which is essentially unchanged compared to that measured for Si/SiO₂ substrate (~64 mV/dec). The selectivity of the graphene ISFET on PET, with respect to Ca²⁺ and Na⁺ ions, also turns out to be very similar to that observed for the ISFET on SiO₂/Si substrate. Both the selectivity and sensitivity results clearly indicate the strong promise of PET substrate for realizing high-performance graphene ISFETs for implantable biosensing applications. The stable performance of GISFETs in different solution or fabricated on different substrates are shown in Fig. 5(c).

4. Conclusions

In conclusion, we have demonstrated a novel ISFET device capable of performing highly sensitive and selective detection of K⁺ ions in various media over a wide ionic concentration range of 1 μM – 20 mM. The sensitivity exhibited by the sensor of 61 ± 4.6 mV/decade over a duration of two months is very comparable to the best Si-based ISFETs available commercially, while the sensor response to interfering Na⁺ and Ca²⁺ ions were found to be negligible. The K⁺ ion detection performance of the sensor remained unaltered in presence of orders of magnitude higher Na⁺ concentrations, and also in Tris-HCl solution, indicating the effectiveness of the sensor for sensing in physiological solutions. The sensor performance also did not change significantly with repeated testing over a period of one month highlighting its robustness and reliability. When fabricated on a PET substrate, the sensor very similar performance, which is highly encouraging for developing flexible bio-implantable graphene-based ISFETs

Acknowledgements

We would like to thank Chuanbing Tang group at the University of South Carolina for performing the synthesizing of the polymer matrix in this research. Financial support for this work from the National Science Foundation (Grants Nos. ECCS-1500007, ECCS-1559711, and ECCS-1512342) is also thankfully acknowledged.

- [1] K. I. Bolotin, K. J. Sikes, J. Hone, H. L. Stormer and P. Kim, Temperature-dependent transport in suspended graphene, *Phys. Rev. Lett.*, 2008, 101, 096802
- [2] F. Schedin, A. K. Geim, S. V. Morozov, E. W. Hill, P. Blake, M. I. Katsnelson, and K. S. Novoselov, Detection of individual gas molecules adsorbed on graphene, *Nat. Mater.*, 2007, 6, 652-5
- [3] O. Akhavan, E. Ghaderi and R. Rahighi, Toward single-DNA electrochemical biosensing by graphene nanowalls, *ACS nano.*, 2012, 6(4), 2904-16
- [4] A. K. Singh, M. A. Uddin, J. T. Tolson, H. Maire-Afeli, N. Sbrockey, G. S. Tompa, M. G. Spencer, T. Vogt, T. S. Sudarshan and G. Koley, Electrically tunable molecular doping of graphene, *Appl. Phys. Lett.*, 2013, 102, 043101
- [5] J. Janata, Historical review. Twenty years of ion-selective field-effect transistors, *Analyst.*, 1994, 119, 2275-8
- [6] L. T. Yin, J. C. Chou, W. Y. Chung, T. P. Sun and S. K. Hsiung, Study of indium tin oxide thin film for separative extended gate ISFET, *Mater. Chem. Phys.*, 2001, 70, 12-6
- [7] O. Devinsky, A. Vezzani, S. Najjar, N. C. De Lanerolle and M. A. Rogawski, Glia and epilepsy: excitability and inflammation. *Trends in neurosciences*, *Trends Neurosci.*, 2013, 36, 174-84.
- [8] M. Rubart and D. P. Zipes, Mechanisms of sudden cardiac death, *The Journal of clinical investigation*, 2005, 115, 2305-15

- [9] A. Topkar and R. Lal, Effect of electrolyte exposure on silicon dioxide in electrolyte-oxide-semiconductor structures, *Thin Solid Films*, 1993, 232, 265-70
- [10] S. Libertino, S. Conoci, A. Scandurra and C. Spinella, Biosensor integration on Si-based devices: Feasibility studies and examples, *Sens. Actuators, B*, 2013, 179, 240-51
- [11] M. A. Uddin, A. K. Singh, T. S. Sudarshan and G. Koley, Functionalized graphene/silicon chemi-diode H₂ sensor with tunable sensitivity, *Nanotechnol.*, 2014, 25, 125501.
- [12] C. C. Cid, J. Riu, A. Maroto and F. X. Rius, Ion-sensitive field effect transistors using carbon nanotubes as the transducing layer, *Analyst*, 2008, 133, 1001-4
- [13] L. Y. Heng and E. A. Hall, Methacrylic-acrylic polymers in ion-selective membranes: achieving the right polymer recipe, *Anal. Chim. Acta.*, 2000, 403, 77-89
- [14] C. Z. Lai, M. M. Joyer, M. A. Fierke, N. D. Petkovich, A. Stein and P. Bühlman, Subnanomolar detection limit application of ion-selective electrodes with three-dimensionally ordered macroporous (3DOM) carbon solid contacts, *J. Solid State Electrochem.*, 2009, 13, 123
- [15] R. He and T. Kyu, Effect of Plasticization on Ionic Conductivity Enhancement in Relation to Glass Transition Temperature of Crosslinked Polymer Electrolyte Membranes, *Macromolecules.*, 2016, 5637-48.
- [16] T. Masadome, T. T. Kie, S. I. Wakida and K. Higashi, Evaluation of effect of additive salts on response of potassium-selective neutral carrier based electrodes using ion-sensitive field-effect transistor, *Anal. Commun.*, 1997, 34, 389-90
- [17] O. H. LeBlanc Jr and W. T. Grubb, Long-lived potassium ion selective polymer membrane electrode, *Anal. Chem.*, 1976, 48, 1658-60
- [18] P. D. van der Wal, E. J. Sudhölter, B. A. Boukamp, H. J. Bouwmeester and D. N. Reinhoudt, Impedance spectroscopy and surface study of potassium-selective silicone rubber membranes, *J. Electroanal. Chem. Interfacial Electrochem.*, 1991, 317, 153-68
- [19] M. C. Rose and R. W. Henkens RW, Stability of sodium and potassium complexes of valinomycin, *Biochim. Biophys. Acta*, 1974, 372, 426-35.
- [20] T. E. Andreoli, M. Tieffenberg and D. C. Tosteson, The effect of valinomycin on the ionic permeability of thin lipid membranes, *J. Gen. Physiol.*, 1967, 50, 2527-45
- [21] W. Fu, C. Nef, O. Knopfmacher, A. Tarasov, M. Weiss, M. Calame and C. Schönenberger, Graphene transistors are insensitive to pH changes in solution, *Nano Lett.*, 2011, 11, 3597-600.
- [22] B. Wang, K. L. Liddell, J. Wang, B. Koger, C. D. Keating and J. Zhu, Oxide-on-graphene field effect bio-ready sensors, *Nano Res.*, 2014, 7, 1263-70
- [23] I. Fakih, S. Sabri, F. Mahvash, M. Nannini, M. Sijaj and T. Szkopek, Large area graphene ion sensitive field effect transistors with tantalum pentoxide sensing layers for pH measurement at the Nernstian limit, *Appl. Phys. Lett.*, 2014, 105, 083101
- [24] W. Fu, C. Nef, A. Tarasov, M. Wipf, R. Stoop, O. Knopfmacher, M. Weiss, M. Calame and C. Schönenberger, High mobility graphene ion-sensitive field-effect transistors by noncovalent functionalization, *Nanoscale*, 2013, 5, 12104-10.
- [25] D. W. Boukhvalov and M. I. Katsnelson, Chemical functionalization of graphene, *J. Phys.: Condens. Matter*, 2009, 21, 344205
- [26] A. C. Ferrari, Raman spectroscopy of graphene and graphite: disorder, electron-phonon coupling, doping and nonadiabatic effects, *Solid State Commun.*, 2007, 143(1):47-57.
- [27] L. M. Malard, M. A. Pimenta, G. Dresselhaus and M. S. Dresselhaus, Raman spectroscopy in graphene, *Physics Reports*, 2009, 473, 51-87.
- [28] A. Singh, M. Uddin, T. Sudarshan and G. Koley, Tunable Reverse - Biased Graphene/Silicon Heterojunction Schottky Diode Sensor, *Small*. 2014, 10, 1555-65
- [28] M. A. Uddin, Y. Zhu, A. Singh, H. Li, M. S. Islam, G. Koley, Effect of epoxy exposure on the electronic properties of graphene, *J. Phys. D: Appl. Phys.*, 2016, 49, 46LT02
- [30] S. Chen, Z. B. Zhang, L. Ma, P. Ahlberg, X. Gao, Z. Qiu, D. Wu, W. Ren, H. M. Cheng and S. L. Zhang, A graphene field-effect capacitor sensor in electrolyte, *Appl. Phys. Lett.*, 2012, 101, 154106
- [31] M. A. Uddin, N. Glavin, A. Singh, R. Naguy, M. Jespersen, A. Voevodin and G. Koley, Mobility enhancement in graphene transistors on low temperature pulsed laser deposited boron nitride, *Appl. Phys. Lett.*, 2015, 107, 203110
- [32] J. L. Qi, K. Nagashio, T. Nishimura, A. Toriumi, The crystal orientation relation and macroscopic surface roughness in hetero-epitaxial graphene grown on Cu/mica, *Nanotechnol.*, 2014, 25, 185602

- [33] J. Ye, M. F. Craciun, M. Koshino, S. Russo, S. Inoue, H. Yuan, H. Shimotani, A. F. Morpurgo and Y. Iwasa, Accessing the transport properties of graphene and its multilayers at high carrier density, *Proc. Natl. Acad. Sci. U.S.A.*, 2011, 108, 13002-6
- [34] T. K. Truong, T. N. Nguyen, T. Q. Trung, I. Y. Sohn, D. J. Kim, J. H. Jung and N. E. Lee, Reduced graphene oxide field-effect transistor with indium tin oxide extended gate for proton sensing, *Curr. Appl. Phys.*, 2014, 14, 738-43
- [35] N. Nikkhoo, P. G. Gulak and K. Maxwell, Rapid detection of E. coli bacteria using potassium-sensitive FETs in CMOS, *IEEE Trans. Biomed. Circuits Syst.*, 2013, 7, 621-30
- [36] K. B. Walsh, N. DeRoller, Y. Zhu and G. Koley, Application of ion-sensitive field effect transistors for ion channel screening, *Biosens. Bioelectron.*, 2014, 54, 448-54
- [37] C. Jimenez, A. Bratov, N. Abramova and A. Baldi, ISFET based sensors: fundamentals and applications, *Encycl. Sens.*, 2006, 151-96
- [38] R. A. Durst and B. R. Staples, Tris/Tris· HCl: A standard buffer for use in the physiologic pH range, *Clinical Chem.*, 1972, 18, 206-8.
- [39] Z. Chen and J. Appenzeller, Mobility extraction and quantum capacitance impact in high performance graphene field-effect transistor devices, *IEDM*, 2008, 1-4
- [40] J. Leadbitter, P. Tice, D. Ottenio, J. Y. Escabasse and B. Podd, Packaging materials: 1. Polyethylene terephthalate (PET) for food packaging applications, *Int. Life Sci.*, 2000, 16. ISBN 1-57881-092-2
- [41] G. Schwartz, B. C. Tee, J. Mei, A. L. Appleton, D. H. Kim, H. Wang and Z. Bao, Flexible polymer transistors with high pressure sensitivity for application in electronic skin and health monitoring, *Nat. Commun.*, 2013, 4, 1859